Quantum confinement and negative heat capacity

2013 EPL 104 16004

(http://iopscience.iop.org/0295-5075/104/1/16004)

A Letters Journal Exploring the Frontiers of Physics

October 2013

EPL, **104** (2013) 16004 www.epljournal.org
doi: 10.1209/0295-5075/104/16004

Quantum confinement and negative heat capacity

Pablo Serra[1,2], Marcelo A. Carignano[1], Fahhad H. Alharbi[1,3] and Sabre Kais[1,4]

[1] *Qatar Environment and Energy Research Institute, Qatar Foundation - Doha, Qatar*
[2] *Facultad de Matemática, Astronomía y Física, Universidad Nacional de Córdoba and IFEG-CONICET Ciudad Universitaria, X5016LAE Córdoba, Argentina*
[3] *King Abdulaziz City for Science and Technology - Riyadh, Saudi Arabia*
[4] *Department of Chemistry, Physics and Birck Nanotechnology Center, Purdue University West Lafayette, IN 47907 USA*

received 5 July 2013; accepted in final form 2 October 2013
published online 28 October 2013

PACS 65.80.-g – Thermal properties of small particles, nanocrystals, nanotubes, and other related systems
PACS 68.65.-k – Low-dimensional, mesoscopic, nanoscale and other related systems: structure and nonelectronic properties
PACS 65.90.+i – Other topics in thermal properties of condensed matter

Abstract – Thermodynamics dictates that the specific heat of a system is strictly non-negative. However, in finite classical systems there are well-known theoretical and experimental cases where this rule is violated, in particular finite atomic clusters. Here, we show for the first time that negative heat capacity can also occur in finite quantum systems. The physical scenario on which this effect might be experimentally observed is discussed.

Thermodynamics dictates that the specific heat of a system is strictly non-negative, implying that the addition (subtraction) of energy cannot result in a decrease (increase) of the system's temperature [1]. Nevertheless there are well-known cases where this rule is apparently violated [2,3]. Systems in weak contact with a thermal bath, which are described by the Canonical ensemble, may not have a negative heat capacity. Systems that are not included in this condition, such as isolated systems that have to be described by the Microcanonical ensemble, may display negative heat capacity. For example, Schmidt *et al.* measured, in an elegant series of experiments, the negative heat capacity of a Na cluster with 147 atoms for temperatures neighboring the melting temperature of the cluster [4–6].

The origin of the negative heat capacity in clusters has been extensively examined by Berry and coworkers [7–12], and other isolated classical systems have been studied by Campisi *et al.* [13] and by Dunkel and Hilbert [14,15]. Other examples of negative heat capacity can be found in the literature, such as strongly coupled open quantum systems [16,17] and dissipative quantum systems [18,19]. At the astronomical scale negative heat capacities have been known for years [20], where it is observed that stars and star clusters increase their temperature as they age while losing energy by radiation [21]. Therefore, invoking the thermodynamic limit is not sufficient to guarantee the equivalence of Canonical and Microcanonical ensembles. The key to theoretically reconcile these results with the thermodynamics was addressed by Thirring and coworkers: A system may display negative heat capacity, even in the thermodynamics limit, provided that it is not ergodic [22–24].

In this letter we investigate whether this phenomenon could also be observed in the quantum domain, in particular, for a small isolated system described within the Microcanonical formalism. Following previous ideas [25,26] on a minimal model having negative specific heat for classical systems we study the effect of the delocalization of the wave function on the average kinetic energy of the system, and also on several definitions of temperature corresponding to the Canonical and Microcanonical statistics. Let us consider a 1d potential well trapped between impenetrable walls:

$$V(x) = \begin{cases} -U_0, & \text{if } |x| < a, \\ 0, & \text{if } a \le |x| < L, \\ \infty, & \text{if } |x| \le L. \end{cases} \quad (1)$$

This potential represents a simple example that suffices to show how a negative heat capacity emerges. The solution of the Schrödinger equation for one particle in $V(x)$

given by eq. (1) can be found in ref. [27]. The solution for a system of N non-interacting electrons can be constructed from the one particle solution. The Coulombic correlation effects for $N = 2$ were tested to be very small and therefore neglected in the calculations for higher N. The values for the parameters U_0 and a for the external potential $V(x)$ were selected to approximately represent quantum dots binding energy and size and are specified in the corresponding figures.

Within the Canonical formalism there is no ambiguities to establish the relation between the energy of the different eigenstates and the temperature of the system, and a continuous temperature can be assigned to a Canonical ensemble. However, in the Microcanonical ensemble the situation is different and to the best of our knowledge there is no accepted "recipe" to calculate the temperature corresponding to a particular eigenstate. Since we are considering systems with one or a few degrees of freedom we use the volume or *Hertz* entropy rather the surface or *Boltzmann* entropy [28]. Then here we define the entropy of a small quantum Microcanonical system as $S(E) = k_B \ln \Omega(E)$, where $\Omega(E)$ is the number of states with $E_n \leq E$ and k_B the Boltzmann constant. $S(E)$ is a piecewise constant function that eventually converges, as it will be shown below, to a continuous convex function of the energy as the number of particles goes to infinity. Straightforward application of the thermodynamic definition of temperature, $1/T^{(\mu)} = \partial S/\partial E$, to our definition for $S(E)$ does not produce a finite temperature. However, the general structure of $S(E)$ from different examples suggests that a slope (*i.e.* a temperature) can be derived from this curve. Here we propose to calculate the Microcanonical temperature using finite difference between adjacent states:

$$T^{(\mu)} = \frac{\Delta E_n}{\Delta S_n}. \tag{2}$$

This definition has the disadvantage that it is not unique, since the finite difference could be taken in many different ways, being the forward, backward and centered differences the more usual choices in several fields. Moreover, this definition proves to be useful for $N = 1$ but it becomes noisy for larger N due to the lack of regularity in the energy levels leading to ΔE_n values that vary significantly form one level to the next. Note also that from eq. (2) the temperature results a quantized property of the system, as can be calculated only for the eigenvalues of the system. A second possibility for the definition of the temperature emerges from the kinetic energy operator K, which can be combined with the equipartition theorem to produce

$$T_n^{(K)} = \frac{2}{d}\frac{\langle n|K|n\rangle}{N} = \frac{2}{d}\frac{\langle K\rangle_n}{N}, \tag{3}$$

where $|n\rangle$ represents a pure state of a system of N particles. Certainly, there are few other quantum definitions of the temperature [29,30]. We will use and compare the most noticeable definitions in a following full detailed paper as this will be beyond the scope and the size of this letter.

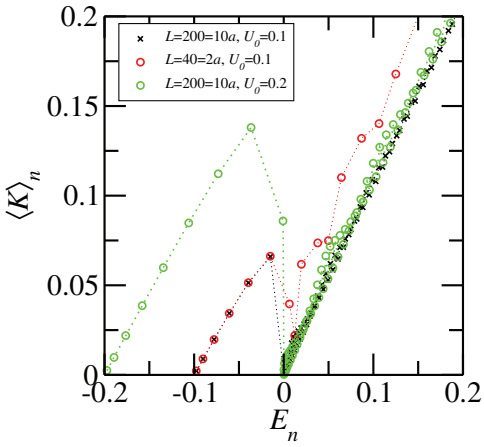

Fig. 1: (Colour on-line) Expectation value of the kinetic energy as a function of the energy for different model parameters. A drop in $\langle K\rangle_n$ occurs as the particle is able to explore regions beyond the central well.

In fig. 1 we show $\langle K\rangle_n$ *vs.* E_n for one particle in the model potential of eq. (1) for three different parameter sets. The parameters displayed in the figure are in atomic units and $a = 1$, and the examples shown correspond to a central confinement region with a diameter of 0.2 nm and 1 nm and a well depth of 2.7 eV and 5.4 eV. This values are representative of multi-layered semiconductor quantum dots [31,32]. All three curves shows the same qualitative feature: as the energy approaches the threshold value to escape from the central well, $\langle K\rangle_n$ decreases implying a negative heat capacity. The magnitude of this effect depends on the depth of the well U_0 that for a fixed a controls the number of bound states and therefore defines the lower energy branch of fig. 1, and the relative delocalization L/a that controls the magnitude of the reduction in kinetic energy as the particle exits the well. This dependence is very similar to what occurs in the classical case. The reason for this becomes clear by looking at the probability density for a particular case. For model potential of the general shape as the one described by eq. (1), the origin of the temperature decrease in the classical problem is the availability of a large space accessible upon the increment of a small amount of energy. In the quantum case the same general picture is valid, with a minor adaptation since a quantum particle is able to penetrate the regions of negative energy due to exponential tail of the wave function. Namely, for a quantum particle the delocalization starts to take place for those eigenstates with E_n slightly smaller than zero. In fig. 2 we show the probability density for the ground state together with the highest state just below the edge of well expansion and lowest state just above that. The probability density of the ground state and the next three states (not shown) are *almost* fully localized in the region $|x| \lesssim a$ and therefore the kinetic energy follows the expected thermodynamic

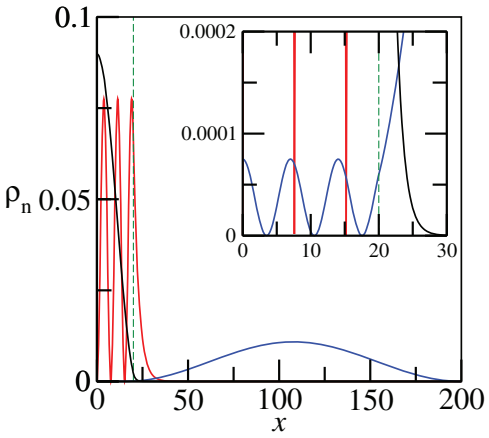

Fig. 2: (Colour on-line) Probability density for $L = 200 = 10a$, $U_0 = 0.1$ for the ground state (black, $E_0 = -0.0975$), highest negative (red, $E_5 = -0.0149$) an lowest positive (blue, $E_6 = 0.000145$).

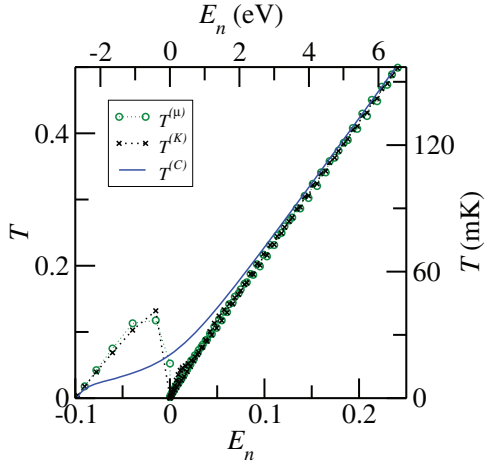

Fig. 3: (Colour on-line) Temperature *vs.* energy for the parameters corresponding to fig. 2. All temperature definitions are equivalent for large energy values. The upper and right axis units are calculated assuming $U_0 = 2.7\,\mathrm{eV}$, $a = 1\,\mathrm{nm}$, $L = 10\,\mathrm{nm}$.

behavior, namely, it linearly increases with the system energy. The highest bounded state (negative energy) shows a small probability to be found for $|x| > a$ and since this region contributes with a much smaller kinetic energy the expectation value $\langle K\rangle_n$ displays a bend departing from the linear relation. The first state with positive energy can explore with no penalty (meaning the wave function is oscillatory, not exponentially decaying) the full available space. This possibility to leave the central well is reflected in a much lower $\langle K\rangle_n$, which in turn imply a negative heat capacity if we directly associate kinetic energy with temperature. Further increase of the energy once the threshold value has been crossed results again in the expected monotonic increase of the kinetic energy. From fig. 1 it can also be observed the emergence of a noise, as an odd-even effect for $E_n > 0$, in particular for the case $L = 200 = 10a$ with $U_0 = 0.2$.

We now compare the predictions of the Microcanonical and Canonical ensembles, $T^{(\mu)}$ and $T^{(C)}$, as well as the temperature defined from the kinetic energy operator $T^{(K)}$. In fig. 3 we show these temperatures corresponding to the case displayed in fig. 2. First we note the remarkable similarity between $T^{(K)}$ and $T^{(\mu)}$. It is important to mention that in the calculation of $T^{(\mu)}$ we have used the centered difference formula. If the forward or backward finite difference derivatives are employed the qualitative results are the same, but those curves display a characteristic odd-even effect that introduce an unnecessary complication. The Canonical temperature $T^{(C)}$ shows the expected thermodynamic behavior as it increases monotonically with the energy of the system, smoothly bridging the low and high-temperature regimes where it matches the other two temperature definitions. Figure 3 clearly shows that a quantum negative heat capacity emerges from the model potential much in the same way that it does for classical systems. The sudden availability of space, accessible upon

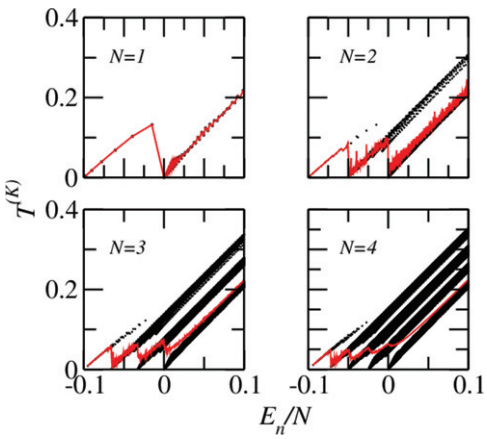

Fig. 4: (Colour on-line) $T^{(K)}$ (black) and $T_I^{(\overline{K})}$ (red) as a function of the energy per particle for systems of with $N = 1$ to $N = 4$. $T_E^{(\overline{K})}$ was calculated using $\epsilon = 0.0004$.

a small increment of the total energy, leads to the decrease of the average temperature of the system.

The question that arises is how this results are affected by increasing the number of particles in the system. The definitions of $T^{(K)}$ and $T^{(\mu)}$ are independent of the system size and therefore may be directly applied to the problem of several particles. In fig. 4 (black) we show $T^{(K)}$ as a function of energy for $N = 1, 2, 3$ and 4. For $N = 1$, $T^{(K)}$ shows only one jump as the particle leaves the central well crossing from a negative to a positive eigenenergy. However for $N > 1$ the kinetic energy shows successive drops and multiple branches as the total energy allows each of the particles to explore the region with positive energies and $|x| > a$. Then, for $N = 2$ there appear two branches in the $T^{(K)}$ *vs.* E curve corresponding to one and two particles with energies greater than zero, respectively. Three branches are present for $N = 3$, corresponding to one,

two and three particles with energies greater than zero, respectively, and so on. The persistence of these branches for large energies is because the system can always reach to a large energy state keeping all but one particle inside the well. Then, the first branch is the resulting kinetic energy from states having only one particle with positive energy. The second branch corresponds to the collection of states having two particles with positive energy, and so on. It is important to note that the entropy corresponding to the different branches is significantly different, with the upper branches corresponding to states with confined particles and lower entropy and the lowermost branch corresponding to the highest entropy. This branching behavior eliminates $T^{(K)}$ as useful generic definition for the temperature of a system. The calculation of the Microcanonical temperature $T^{(\mu)}$, although possible, does not provide a clear vision of the behavior of the system because of the noise introduced by the finite difference method. Then we adopt yet another definition for the temperature that reduces to $T_n^{(K)}$ for $N = 1$, but uses the *quasi*-degeneracy of states with very different kinetic energy to eliminate the branches occurring for $N > 1$. In eq. (3) a temperature is assigned to each eigenstate of the system, even in the case of *quasi*-degeneracy, *i.e.* more than one state with very similar energy and, eventually, very different kinetic energy. Following a textbook development of the Microcanonical ensemble [1], we introduce a small parameter ϵ such that $E_{n+1} - E_n \ll \epsilon$, $\forall n$, and we define the set I_E as

$$I_E = \{i \,|\, E \leq E_i < E + \epsilon\}. \tag{4}$$

where each set will have N_I elements. Then, the state

$$\Psi_E = \sum_{i \in I_E} c_i \psi_i \tag{5}$$

will be a *quasi*-eigenstate with an assigned energy E. Next we calculate the kinetic energy corresponding to the energy E as an average of the kinetic energy over all the normalized *quasi*-degenerate states Ψ_E:

$$\begin{aligned}\overline{K}_E &= \frac{\int \prod_{i\in I_E} \mathrm{d}c_i^* \, \mathrm{d}c_i \delta\left(1 - \sum_{i\in I_E} |c_i|^2\right) \langle \Psi_E \,|K|\, \Psi_E \rangle}{\int \prod_{i\in I_E} \mathrm{d}c_i^* \mathrm{d}c_i \delta\left(1 - \sum_{i\in I_E} |c_i|^2\right)} \\ &= \sum_{n,m\in I_E} K_{m,n} \frac{\int \prod_{i\in I_E} \mathrm{d}c_i^* \mathrm{d}c_i \, c_m^* \, c_n \, \delta\left(1 - \sum_{i\in I_E} |c_i|^2\right)}{\int \prod_{i\in I_E} \mathrm{d}c_i^* \mathrm{d}c_i \, \delta\left(1 - \sum_{i\in I_E} |c_i|^2\right)} \\ &= \frac{1}{N_I} \sum_{m\in I_E} K_{m,m}, \end{aligned} \tag{6}$$

where the integrals are obtained using the Fourier representation of the delta function, and $K_{m,n} = \langle \psi_m \,|K|\, \psi_n \rangle$. The temperature related with the average kinetic energy is defined following eq. (3) as

$$T_E^{(\overline{K})} = \frac{2}{d} \frac{\overline{K}_E}{N}. \tag{7}$$

In fig. 4 we show $T_E^{(\overline{K})}$ as continuous red lines. Note that $T_E^{(\overline{K})}$ coincides with $T^{(K)}$ for $N = 1$, but it does not display branches for $N > 1$. Moreover, $T_E^{(\overline{K})}$ shows a series of temperature drops as each particle has sufficient energy to escape the well and reach the larger region, resulting in N energy intervals with negative specific heat. As the number N of particles increases, the magnitude of the temperature drop becomes smaller and eventually disappear in the thermodynamic limit $N \to \infty$, where $T_E^{(\overline{K})}$ is expected to converge to the Canonical temperature. Finally, notice that the oscillations displayed by $T_E^{(\overline{K})}$ resemble those observed in similar classical models [14,15,26].

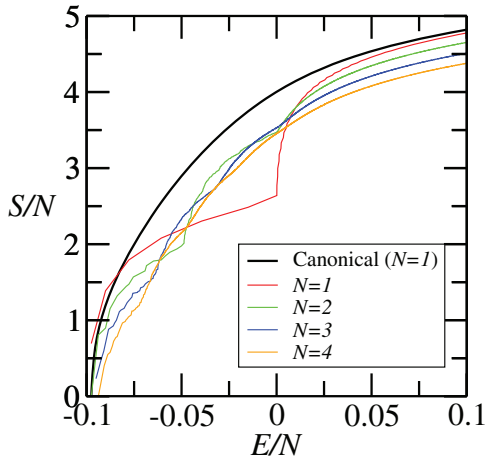

Fig. 5: (Colour on-line) Entropy per particle as a function of the energy per particle for systems with a few particles. Increasing N reduce, and eventually eliminates, the concavity region while approaching the Canonical result.

The Microcanonical entropy calculated by simply counting the number of states also has a clear interpretation. In fig. 5 we show our results for S *vs.* E for systems of up to $N = 4$. The figure also includes the Canonical result. Note that fig. 5 shows the values of quantized entropy connected with straight lines, and as the number of particles increases the noise of the curve is reduced although not enough to result in a smooth curve upon numerical differentiation. For $N = 1$ the entropy shows a concave kink at $E \simeq 0$ that leads to a temperature drop. As N increases, as observed in the behavior of $T_E^{(\overline{K})}$, this kink splits as many times as particles in the system. Each one of these N kinks is weaker than the $N - 1$ kinks of a smaller system. Therefore, it is clear that this kink splitting mechanism will eventually completely remove all the concavities in the S *vs.* E curve as N becomes very large. As a consequence, in the thermodynamic limit, we expect a full equivalence of the Microcanonical and Canonical descriptions. In fact, the Canonical entropy also displayed in fig. 5 is essentially parallel to the Microcanonical entropy for $N = 4$. The fact the the two ensembles are equivalent on the thermodynamic limit is expected since the simple model of eq. (1) does not contains energy barriers that could lead to non-ergodicity, another source of difference between the ensembles.

The physical scenario on which this effect could be experimentally observed in the quantum domain is with quantum confined semiconductor devices, core/shell nanoparticles or even graphene layers [33,34] or nanoribbons [35]. The key ingredient is to have spacial confinement connected with a much wider region, *i.e.* a *localized* and a *delocalized* region, where the access to the second becomes possible upon a small increment of the system's energy. Spatial delocalization can be in principle constructed in multiple quantum wells and wires and core/shell nanoparticles. By proper doping and design, the highly localized states can be occupied and electrons can be excited to the delocalized states by low-energy photons. However, the challenge is how to measure the delocalization effect on the temperature. Carrier temperature has been estimated indirectly and qualitatively using optoelectronic measurements and micro-Raman spectroscopy [36–39].

* * *

The authors would like to acknowledge Prof. Timothy S. Fisher from Purdue University for discussions and his continuing efforts to harness this effect in an experimental system.

REFERENCES

[1] Huang Kerson, *Statistical Mechanics* (John Wiley & Sons, New York) 1987.
[2] Behringer H., Pleimling M. and Hüller A., *J. Phys. A: Math. Gen.*, **38** (2005) 973.
[3] Komatsu N., Kimura S. and Kiwata T., *Phys. Rev. E*, **80** (2009) 041107.
[4] Schmidt M., Kusche R., Kronmüller W., von Issendorff B. and Haberland H., *Phys. Rev. Lett.*, **79** (1997) 99.
[5] Schmidt M., Kusche R., von Issendorff B. and Haberland H., *Nature*, **393** (1998) 238.
[6] Schmidt M., Kusche R., Hippler T., Donges J., Kronmüller W., von Issendorff B. and Haberland H., *Phys. Rev. Lett.*, **86** (2001) 1191.
[7] Berry R. S. and Smirov B. M., *J. Chem. Phys.*, **130** (2009) 064302.
[8] Proykova A. and Berry R. S., *J. Phys. B*, **39** (2006) R167.
[9] Jortner J. and Rosenblit M., *Adv. Chem. Phys.*, **132** (2006) 247.
[10] Berry R. S., *Theor. Chem. Acc.*, **127** (2010) 203.
[11] Berry R. S. and Smirov B. M., *J. Exp. Theor. Phys.*, **98** (2004) 366.
[12] Berry R. S., *Isr. J. Chem.*, **44** (2004) 211.
[13] Campisi M., Zhan F. and Hänggi P., *EPL*, **99** (2012) 60004.
[14] Hilbert S. and Dunkel J., *Phys. Rev. E*, **74** (2006) 011120.
[15] Dunkel J. and Hilbert S., *Physica A*, **370** (2006) 390.
[16] Campisi M., Talkner P. and Hänggi P., *J. Phys. A*, **42** (2009) 392002.
[17] Campisi M., Zueco D. and Talkner P., *Chem. Phys.*, **375** (2010) 187.
[18] Hänggi P. and Ingold G. L., *Acta Phys. Pol. B*, **37** (2006) 1537.
[19] Hänggi P., Ingold G. L. and Talkner P., *New J. Phys.*, **10** (2008) 115008.
[20] Lynden-Bell D. and Wood R., *Mon. Not. R. Astron. Soc.*, **138** (1968) 495.
[21] Lynden-Bell D., *Physica A*, **263** (1999) 293.
[22] Thirring W., *Z. Phys.*, **235** (1970) 339.
[23] Hertel P. and Thirring W., *Ann. Phys. (N.Y.)*, **63** (1971) 520.
[24] Thirring W., Narnhofer H. and Posch H. A., *Phys. Rev. Lett.*, **91** (2003) 130601.
[25] Rao J., Liu Q. H., Liu T. G. and Li L. X., *Ann. Phys. (N.Y.)*, **323** (2008) 1415.
[26] Carignano M. A. and Gladich I., *EPL*, **90** (2010) 63001.
[27] Flügge Siegfried, *Practical Quantum Mechanics* (Springer, Berlin) 1994.
[28] Joshi D. G. and Campisi M., *Eur. Phys. J. B*, **86** (2013) 157.
[29] Person E. M., Halicioglu T. and Tiller W. A., *Phys. Rev. A*, **32** (1985) 3030.
[30] Jellinek J. and Goldberg A., *J. Chem. Phys.*, **113** (2000) 2570.
[31] Ferrón A., Serra P. and Osenda O., *Phys. Rev. B*, **85** (2012) 165322.
[32] Ferrón A., Serra P. and Osenda O., *J. Appl. Phys.*, **113** (2013) 134304.
[33] Aoki M. and Amawashi H., *Solid State Commun.*, **142** (2007) 123.
[34] Singh D., Murthy J. Y. and Fisher T. S., *J. Appl. Phys.*, **110** (2011) 044317.
[35] Han M. Y., Öezyilmaz B., Zhang Y. and Kim P., *Phys. Rev. Lett.*, **98** (2007) 206805.
[36] Ikoma T., Hirakawa K., Hiramoto T. and Odagiri T., *Solid State Electron.*, **32** (1989) 1793.
[37] Ikoma T. and Hiramoto T., in *Granular Nanoelectronics*, edited by Ferry David K., Barker John R. and Jacobini Carlo (Plenum Press) 1991.
[38] Xi Y., Xi J.-Q., Gessmann Th., Shah J. M., Kim J. K., Schubert E. F., Fischer A. J., Crawford M. H., Bogart K. H. A. and Allerman A. A., *Appl. Phys. Lett.*, **86** (2005) 031907.
[39] Todoroki S., Sawai M. and Aiki K., *J. Appl. Phys.*, **58** (1985) 1124.